Journal of Zhejiang University SCIENCE A
ISSN 1009-3095 (Print); ISSN 1862-1775 (Online)
www.zju.edu.cn/jzus; www.springerlink.com
E-mail: jzus@zju.edu.cn

Strength and deformation characteristics of steel fibrous concrete beams

SINGH Bhupinder[†1], SINGH S.P.[†2], KAUSHIK S.K.[1]

([1]*Department of Civil Engineering, Indian Institute of Technology, Roorkee 247 667, India*)

([2]*Department of Civil Engineering, National Institute of Technology, Jalandhar 144 011, India*)

[†]E-mail: bhupifce@iitr.ernet.in; spsingh@nitj.ac.in

Received Mar. 4, 2006; revision accepted Oct. 21, 2006

Abstract: The results of an analytical investigation of the flexural behaviour of Steel Fibre Reinforced Concrete (SFRC) beams are presented. The complete response of the SFRC beams under displacement controlled static loading was obtained using nonlinear Finite Element (FE) techniques implemented with the help of ATENA 2D software. Issues relating to the behaviour of SFRC which have a direct bearing on the FE modelling are discussed with relevance to the software employed for the nonlinear analysis. Constitutive models amenable to numerical analysis for steel fibrous concrete are presented. The structural response throughout the loading regime was captured in terms of the load-deflection behaviour, which in addition to the post-peak response characterized the failure mode of the test beams. The crack patterns at crack initiation and at the end of the tests were also recorded. Experimental results from the specimens of two other investigators were used as control values for this investigation. The response of the specimens of this investigation was evaluated in terms of initial tangent stiffness, peak loads and toughness. Good match was obtained between the results from this investigation and corresponding experimentally obtained values, wherever available. The influence of the fibre content is reflected in the observed trends in peak loads, deflection at peak loads and toughness, which are in broad agreement with known behavioral patterns of SFRC.

Key words: Analysis, Deformation, Strength, Steel Fibre Reinforced Concrete (SFRC), Toughness
doi:10.1631/jzus.2007.A0257 **Document code:** A **CLC number:** TU502^{+}.3

INTRODUCTION

Finite Element (FE) procedures are at present widely used in engineering modelling and analysis and employed extensively in the analysis of solids and structures and heat transfer and fluids (Bathe, 1996). The essence of FE solution of an engineering problem is that a set of governing algebraic equations is established which are then solved with the help of a digital computer. The first practical FE procedures were employed in linear analysis of solids and structures (Bathe, 1996), with the implicit assumption being that the structures or bodies under consideration are elastic and obey Hooke's Law throughout the loading regime. From the early 1960s, extensive research and development were carried out to study the effects of steel fibres on the mechanical properties of concrete. Model testing can undoubtedly give insight into structural behaviour, but can be a very costly and time consuming procedure. Therefore, several numerical methods have been developed to predict the structural response of fibrous concrete members (Al-Tann and Ezzadeen, 1992). In this study 2D plane stress analysis was carried out using ATENA 2D software (http://www.cervenka.cz) incorporating a numerical procedure based on FE analysis, for obtaining the complete flexural response of fibrous concrete beams under statically applied loads. Nonlinear analysis is imperative for evaluating structural response in terms of complete load-deflection characteristics, ductility, toughness, mode of failure, etc.

MODELLING

The objective of this investigation is to analytically examine the flexural response of steel fibrous concrete beams to monotonically increasing four-point static loads. For this purpose, 100 mm×100 mm×500 mm prismatic beam specimens were chosen for modelling since the same specimen size was employed by previous investigators (Singh and Kaushik, 1999; Mohammadi and Kaushik, 2001) with whose results those from the present investigation were to be benchmarked. The details of the test specimens and experimental results obtained by the above investigators are summarized in Table 1. For convenience, the experimental control specimens were divided into two groups. In the first group (Singh and Kaushik, 1999) consisting of specimens S1, S2 and S3, the fibre type and aspect ratio was constant, the fibre volume fraction varied from 0.5% to 1.0% and then to 1.5% respectively. In the second group (Mohammadi and Kaushik, 2001) consisting of specimens S4, S5 and S6, the fibre volume fraction was constant and mixed aspect ratio of fibres was employed. The fibre mix ratio by weight varied from 100%:0%, 50%:50% and 0%:100% of the longer and shorter fibres respectively. It may be pointed out that concrete matrix mix proportions of control specimens of the above groups are different and given in Table 1.

Section properties

A simply supported beam as shown in Fig.1, under four point bend test, like the experimental set-up, was selected for analysis. Due to symmetry in geometry and loading conditions, half of the beam with appropriate boundary conditions was considered for analysis. Six specimens in all, each corresponding to one of the control specimens presented in Table 1, were analysed using ATENA 2D software. Four 16 mm nodded quadrilateral elements were used for modelling the fibrous concrete beams. These are isoparametric elements integrated using Gaussian integration at four or nine integration points for the case of bi-linear or bi-quadratic interpolation.

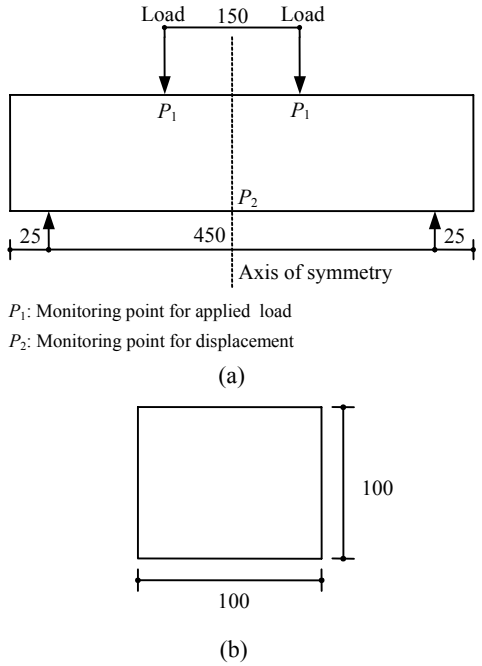

Fig.1 Dimensions and loading details of the analytical test specimen (all dimensions in mm). (a) Elevation; (b) Section

Table 1 Experimentally obtained results (Singh and Kaushik, 1999; Mohammadi and Kaushik, 2001)

Investigator	Specimen designation	Volume fraction (%)	Fibre details	Cube compressive strength (MPa)	Flexural strength (MPa)	Splitting tensile strength (MPa)	Peak load in flexure (kN)
Singh and Kaushik (1999)	S1	0.5	M1	53.37	5.83	4.12*	12.97
	S2	1.0	M1	55.45	6.80	4.80*	15.08
	S3	1.5	M1	56.09	9.03	6.38*	20.06
Mohammadi and Kaushik (2001)	S4	1.0	M2	59.80	7.53	4.82+	15.73
	S5	1.0	M3	62.89	7.51	4.65+	16.68
	S6	1.0	M4	69.83	6.68	4.58+	14.84

M1: Corrugated steel fibres of size 2.0 mm×0.6 mm×30 mm; M2: Corrugated steel fibres 100% long fibres (2 mm×0.6 mm×50 mm)+0% short fibres (2 mm×0.6 mm×25 mm); M3: Corrugated steel fibres 50% long fibres (2 mm×0.6 mm×50 mm)+50% short fibres (2 mm×0.6 mm×25 mm); M4: Corrugated steel fibres 0% long fibres (2 mm×0.6 mm×50 mm)+100% short fibres (2 mm×0.6 mm×25 mm); Mix Proportion for concrete with fibre detail M1—C:F.A:C.A.=1:1.52:1.88, W/C=0.46; Mix proportion for concrete with fibre detail M2, M3, M4—C:F.A:C.A.=1:1.35:21.2, W/C=0.35; * Computed from flexural strength using expression of Lok and Pei (1999); + Experimentally reported values; All specimens were of size 100 mm×100 mm×500 mm

In a typical experimental set-up, the post-peak response of a structural member can be captured only if strain or displacement controlled application of the load is properly achieved for which the testing machine must be sufficiently rigid (Pillai and Menon, 1998). Since the evaluation of the post-peak response of the fibrous concrete beams under investigation was imperative for studying their ductility characteristics, a displacement controlled load application at the rate of 5×10^{-7} m per load step was specified at the point of load application in the software programmed to subject each of the test beams to at least 550 such load steps, which were deemed sufficient to capture the complete response of the specimens under investigation.

Constitutive law for fibrous concrete

The FE equilibrium equations contain the displacement and strain-displacement matrices plus the constitutive matrix of the material. Therefore, in order for a formulation to be applicable to a certain response prediction, both the kinematic and constitutive descriptions must be appropriate. Most FE studies consider concrete to act like an elasto-plastic solid in compression and like an elastic-brittle material in tension. Various elasticity and plasticity based models have been proposed for uncracked concrete. Two different approaches are usually employed for modelling cracking of concrete. The more popular procedure and the one adopted in ATENA, are to treat the cracking as distributed cracks on the continuum level that is, the cracks are speared out in a continuous fashion. The material model for concrete employed in ATENA incorporates the following effects of concrete behaviour viz. nonlinear behaviour in compression including hardening and softening, fracture of concrete in tension based on nonlinear fracture mechanics, biaxial strength failure criteria, reduction of compressive strength after cracking, tension stiffening effect and reduction of shear stiffness after cracking. The contribution of fibres to the strength and pre-peak behaviour of fibrous concrete in compression is relatively small and hence can be neglected without significant loss of accuracy. Hence, the nominal gain in compressive strength due to addition of steel fibres to the matrix is ignored and the initial tangent modulus adopted for SFRC is the same as that for non-fibrous concrete. The ascending portion of the stress-strain curve of fibrous concrete in compression was modelled using the following equations suggested by CEB-FIP Model Code (1990) (Figs.2 and 3).

$$\sigma_c^{ef}=f_c'^{ef}\frac{kx-x^2}{1+(k-2)x}, \tag{1}$$

$$x=\varepsilon/\varepsilon_c, \tag{2}$$

$$k=E_o/E_c, \tag{3}$$

where, σ_c^{ef} is the concrete compressive stress, $f_c'^{ef}$ is the concrete effective compressive strength based on Kupfer *et al*.(1969)'s biaxial failure stress criterion, ε is concrete strain, ε_c is concrete strain at peak stress, x is the normalized strain, k is a shape parameter which can have any value greater than or equal to 1 as for example, if k=1 a linear ascending branch is obtained and if k=2 a parabolic ascending branch is obtained.

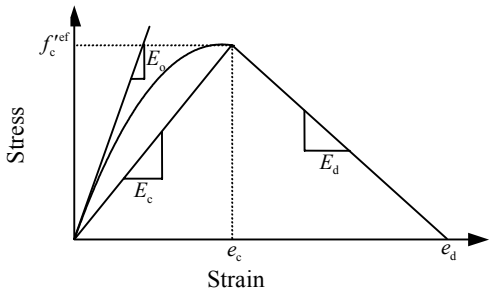

Fig.2 Fibrous concrete stress-strain curve in compression
E_0: the hardening tangent modulus of concrete; E_c: the secant modulus of concrete; e_c: the strain corresponding to peak stress; E_d: the softening modulus of concrete; e_d: the failure strain of concrete

The softening law in compression for fibrous concrete has been assumed to be linearly descending as shown in Fig.3. In general, the softening response can be quantified either in terms of the end point plastic displacement or in terms of the softening modulus or in terms of the angle made by the linearised-softening branch of the stress-strain curve with the horizontal at the peak load. For the purpose of this investigation, the softening response was quantified in terms of end point plastic displacement, w_d. A value of w_d equal to 0.5 mm was adopted for the purpose of this investigation for fibrous concrete (van Mier, 1986). The behaviour of uncracked fibrous concrete in tension has been assumed to be linearly elastic and effective tensile strength was derived from bi-axial failure criterion. To model the post-cracking

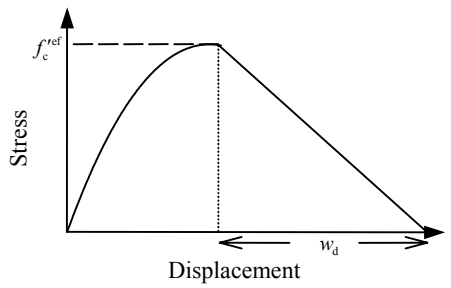

Fig.3 Softening law for fibrous concrete in compression

tensile response of fibrous concrete, a fictitious crack model based on an experimental crack opening law and fracture energy concepts was employed, as shown in Fig.4 (Hordijk, 1991), where w_c is the crack opening at the complete release of stress, $f_t'^{ref}$ is the effective tensile strength of fibrous concrete equal to the split cylinder tensile strength where reported and where the same was not available and calculated from the flexural tensile strength using the following expression given by Lok and Pei (1999),

$$f_t=f_{cr}/1.416. \quad (4)$$

where f_t is the tensile strength of fibrous concrete and f_{cr} is the flexural tensile strength of fibrous concrete.

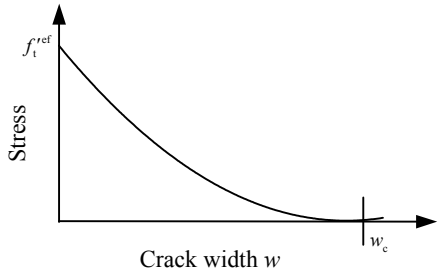

Fig.4 Softening law for fibrous concrete in tension (Hordijk, 1991)

SOLUTION STRATEGIES

The overall effectiveness of an analysis depends to large degree on the numerical procedure used for the solution of the FE equilibrium equations. The most frequently used iteration schemes for solving nonlinear FE equations are Newton-Raphson iteration and other closely related techniques. The basic equations to be solved in nonlinear analysis at time $t+\delta t$ are ${}^{t+\delta t}\boldsymbol{R}-{}^{t+\delta t}\boldsymbol{F}=0$, where the vector ${}^{t+\delta t}\boldsymbol{R}$ stores the externally applied nodal loads and ${}^{t+\delta t}\boldsymbol{F}$ is the vector of the nodal point forces that are equivalent to the element stresses. The Newton-Raphson solution of this equation, as illustrated in Fig.5, is an incremental analysis performed with time or load steps. A characteristic of this iteration is that a new tangent stiffness matrix is calculated at each iteration, the iteration procedure being continued until appropriate convergence criteria are satisfied. Newton-Raphson solution was employed in the software used in this analysis.

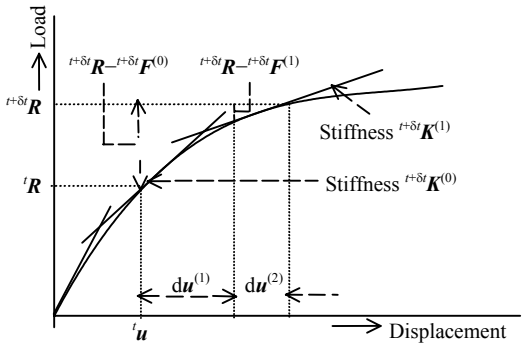

Fig.5 Illustration of Newton-Raphson iteration in solution of single degree of freedom system (Bathe, 1996)

Fig.6 shows the automatic FE meshing executed using four noded isoparametric quadrilateral elements for a typical beam used in the analysis.

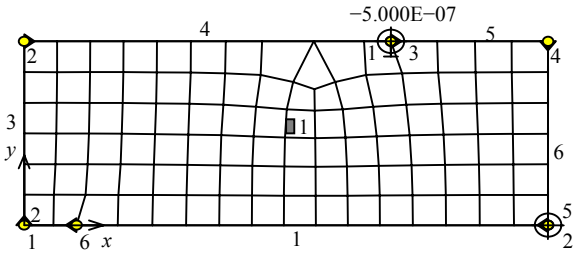

Fig.6 FE mesh for a typical test beam

RESULTS AND DISCUSSION

All the test beams were subjected to 550 load steps, every step entailing a displacement of 5×10^{-7} m, on a personal computer. The behaviour of the beams was captured in terms of the applied load versus the vertical displacement at the mid-span and crack patterns, etc. The incorporation of steel fibres in concrete

is known to have significant effect on the post-peak response of concrete. The post-peak responses of the test specimens of this analysis were evaluated in terms of toughness, defined as area under the load-deflection curve up till the end of the prescribed load steps.

Comparison of analytically obtained load-deflection curves for specimens S1, S2, S3 and specimens S4, S5, S6 is represented in Fig.7a and Fig.7b, respectively. Further, some typical analytically obtained crack patterns at different stages of loading for the specimens S2 and S5 are presented in Figs.8 and 9 respectively, for the purpose of illustration. The test results obtained from this analysis are summarized in Table 2, where experimentally obtained peak loads are compared with those obtained analytically from the present investigation.

Study the load-deflection curves for the specimens of this investigation reveals that, as expected, the response is linear up to peak load and thereafter the post-peak regime is characterized by varying degrees of softening. The influence of fibre characteristics in terms of fibre content expressed as volume fraction can be observed in the values of the peak loads and the deflection under peak load for different test specimens. The energy absorption characteristics of the test specimens are quantified in terms of toughness, measured as area under the load-deflection diagram. A perceptible trend in the variation of toughness of the test specimen vis-à-vis fibre volume fraction is reflected in the results from this investigation.

The analytical and corresponding experimentally obtained peak loads of the test specimens are

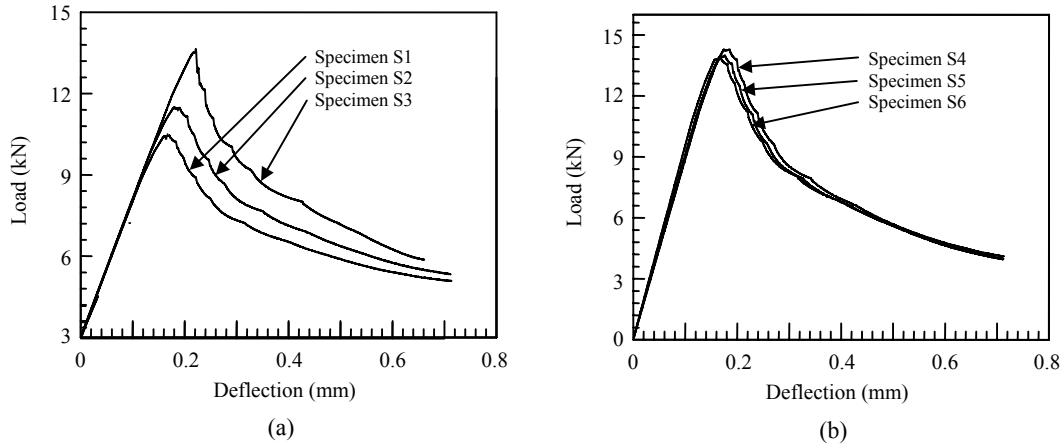

Fig.7 Analytically obtained load-deflection curves. (a) Specimens S1~S3; (b) Specimens S4~S6

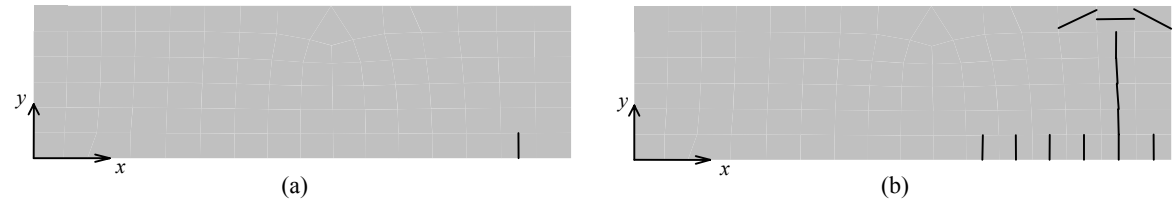

Fig.8 Analytically obtained crack patterns for specimen S2. (a) At crack initiation; (b) At the end of load step 550

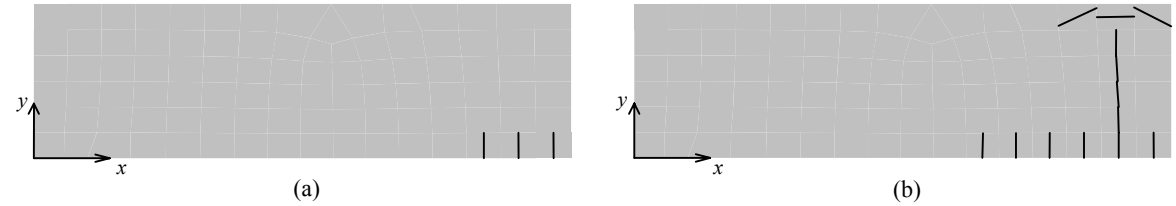

Fig.9 Analytically obtained crack patterns for specimen S5. (a) At crack initiation; (b) At the end of load step 550

compared in Table 2. The analytically obtained values of the peak loads for the first group of specimens i.e. S1, S2 and S3 are 12.40, 14.15 and 17.70 kN respectively whereas, for specimens of the second group i.e. S4, S5 and S6, these values are 14.28, 13.98 and 13.90 kN respectively. It can be observed from Table 2 that good match is obtained between the analytically and experimentally obtained values of the peak load for various specimens tested in this investigation. In general, the analytically obtained peak loads were underestimated 6% to 13% for all the specimens tested in this investigation except specimen S5, where it is up to 19%. This difference in the experimentally and analytically obtained peak loads is quite acceptable.

The characteristics of the ascending portion of the load deflection diagram were captured in terms of initial tangent stiffness, measured as the slope of the linear ascending portion. As can be observed from Table 2, for all the specimens tested in this investigation, the values of the initial tangent stiffness were more or less the same. It may be added that for specimens S1, S2, S3 the direct tensile strength for the purpose of analysis was computed from experimentally obtained flexural strength (Lok and Pei, 1998) of the corresponding specimens, whereas, for the specimens S4, S5 and S6, the tensile strength required for the analysis was available from experimental results (Mohammadi and Kaushik, 2001) and hence was not computed from flexural strength.

Besides their contribution in enhancing the peak load of fibrous concrete, equal or perhaps greater significance is the role of the steel fibres in modifying the pot-peak response and the matrix's mode of failure. A quantitative measure of the energy observing capacity of the matrix is in terms of toughness evaluated as area under the load-deflection curve. For the purpose of this analysis, the toughness was computed as the area under the load-deflection diagram up to the end of load step 550 and the same is summarized in Table 2. It could be observed that as the fibre content increased from 0.5% to 1.0% and then to 1.5% in specimens S1, S2 and S3 respectively, the values of toughness improved from 4.45×10^{-3} kN·m to 4.98×10^{-3} kN·m and then to 5.52×10^{-3} kN·m respectively. Hence, the expected improvement in the energy absorption capacity of the matrix consequent to the increase in volume fraction of fibres is well reflected in the results obtained from analysis. For the specimens of the second group namely S4, S5 and S6 having the same volume fraction of fibres and comparable values of tensile strengths, no discernable trend was observed in toughness values, with the corresponding calculated values of toughness being 5.53×10^{-3}, 5.29×10^{-3} and 5.11×10^{-3} kN·m, respectively. Further, it can be seen from Fig.7a that with the increase in fibre content from 0.5% to 1.0% and then to 1.5% in specimens S1, S2 and S3 respectively, there is significant increase in the deflection at peak load. Larger peak load deflections obviously imply greater energy absorption capacity of the specimen. There is not much difference in the behaviour of specimens S4, S5 and S6 as these specimens incorporate the same volume fraction of fibres and has comparable tensile strengths (Fig.7b).

More or less similar crack patterns were obtained analytically for all the specimens of this investigation. In general, at the initial stages of the test, a series of closely spaced vertical cracks were observed at the soffit of the test beams. At later stages of the test, one of cracks, invariably located in the middle third of the span, moved more or less vertically towards the compression zone of the test beams, culminating in the failure of the specimens. Similar failure mode was observed during experimental

Table 2 Analytically obtained results

Specimen	Volume fraction (%)	Fibre details	Peak load in flexure		P_{ex}/P_{an}	Initial tangent stiffness ($\times10^3$ kN/m)	Toughness ($\times10^{-3}$ kN·m)
			Experimental (P_{ex}) (kN)	Analytical (P_{an}) (kN)			
S1	0.5	M1	12.97	12.40	1.05	88.65	4.45
S2	1.0	M1	15.08	14.15	1.07	89.00	4.98
S3	1.5	M1	20.06	17.70	1.13	88.55	5.52
S4	1.0	M2	15.73	14.28	1.10	88.88	5.53
S5	1.0	M3	16.68	13.98	1.19	88.45	5.29
S6	1.0	M4	14.84	13.90	1.07	88.45	5.11

testing of the specimens. The analytically obtained crack patterns for the specimens S2 and S5, for the purpose of illustration are presented in Figs.8 and 9 respectively. The maximum crack width and number of cracks at the soffit of each specimen tested are presented in Table 3.

Table 3 Maximum crack widths and number of cracks in test specimens

Specimen	Volume fraction (%)	Fibre details	Number of cracks at the soffit of specimen (at the end of load step 550)		Maximum crack width ($\times10^{-4}$ m)
			Minor cracks	Major cracks	
S1	0.5	M1	5	1	1.468
S2	1.0	M1	5	1	1.453
S3	1.5	M1	4	1	1.417
S4	1.0	M2	5	1	1.457
S5	1.0	M3	5	1	1.462
S6	1.0	M4	5	1	1.461

CONCLUSION

Nonlinear FE analysis of SFRC beams was carried out using ATENA 2D software. Constitutive models amenable to numerical analysis for steel fibrous concrete have been presented. Comparison of the results from the present investigation with the experimentally obtained results of the control specimens, wherever available, revealed that the response of the steel fibrous concrete beams could be faithfully captured to a significant degree of accuracy with the use of nonlinear FE analysis techniques implemented using ATENA 2D software. The response has been obtained in terms of load-deflection curves, crack patterns etc. and the behaviour was quantified in terms of initial tangent stiffness and toughness values. The trends observed in the response parameters are in broad agreement with known behavioral patterns.

References

Al-Tann, S.A., Ezzadeen, N.A., 1992. Non-Linear Finite Element Analysis of Steel Fibre Reinforced Members. *In*: Swamy, R.N. (Ed.), Fibre Reinforced Cement and Concrete. E & F N Spon, London, p.435-446.

Bathe, K.J., 1996. Finite Element Procedures. Prentice-Hall of India Pvt. Ltd., New Delhi, p.1037.

CEB-FIP Model Code, 1990. First Draft, Comite Euro-International du Beton, Bulletin d'information No. 195, 196, Mars.

Hordijk, D.A., 1991. Local Approach to Fatigue of Concrete. Ph.D Thesis, Delft University of Technology, the Netherlands.

Kupfer, H., Hilsdorf, H.K., Rusch, K., 1969. Behaviour of concrete under biaxial stress. *Proceedings of ACI*, **66**(8):656-666.

Lok, T., Pei, J., 1999. Flexural behaviour of steel fibre reinforced concrete. *Journal of Materials in Civil Engineering, ASCE*, **10**(2):86-97. [doi:10.1061/(ASCE)0899-1561(1998)10:2(86)]

Mohammadi, Y., Kaushik, S.K., 2001. Steel Fibre Reinforced Concrete with Mixed Aspect Ratio. SEC-2001, Department of Civil Engineering, Phoenix Publishers, IIT Roorkee, p.326-334.

Pillai, S.U., Menon, D., 1998. Reinforced Concrete Design. Tata McGrae-Hill Pub. Co. Ltd., New Delhi, p.762.

Singh, S.P., Kaushik, S.K., 1999. Flexural Fatigue Behaviour of Steel Fibre Reinforced Concrete. CSIR Research Report, New Delhi, p.105.

van Mier, J.G.M., 1986. Multi-Axial Strain Softening of Concrete Part 1: Fracture. *In*: Materials and Structures. RILEM.